Available online at www.sciencedirect.com
SCIENCE DIRECT
Polymer 46 (2005) 513–521
polymer
www.elsevier.com/locate/polymer

# 'Intermediate phase' in poly(ethylene) as elucidated by the WAXS. Analysis of crystallization kinetics

Paweł Sajkiewicz[a,*], Takeji Hashimoto[b], Kenji Saijo[b], Arkadiusz Gradys[a]

[a]*Institute of Fundamental Technological Research, Polish Academy of Sciences, Świętokrzyska 21, 00-049 Warszawa, Poland*
[b]*Department of Polymer Chemistry, Kyoto University, Kyoto 615-8510, Japan*

Received 7 May 2004; received in revised form 4 November 2004; accepted 8 November 2004
Available online 30 November 2004

**Abstract**

The analysis of WAXS profiles for various polyethylenes indicates that the proper description of a structure needs the introduction of a kind of 'third phase' in addition to the classical crystalline and amorphous phases. The structure of the additional phase is intermediate between that of the amorphous and crystalline phase. With increasing branch content and molecular weight the intermediate phase becomes more similar to the structure of amorphous phase. The experimental evidence for the intermediate phase is derived not only from the crude approximation of WAXS profiles based on the two phase model but also from the unexpected behavior of the parameters of amorphous halo during crystallization. When crystallization is started, an analysis based upon two-phase model results in an apparent increase of the diffraction angle and width of amorphous halo with time above the values anticipated from the range before the start of crystallization. This is caused by the fact that the amorphous fitting function tries to cover a peak of the intermediate component that appears between amorphous halo and (110) reflection of crystalline phase. The conventionally applied two-phase model leads to several serious errors in determination of structural parameters of both phases.

The analysis of crystallization kinetics using three-phase model provides additional information on the nature of crystallization itself.


*Keywords:* Polyethylene; Crystallization; Intermediate phase

## 1. Introduction

In the frame of traditional analysis, polymers are semicrystalline materials composed of two phases: crystalline and amorphous. This classical model of polymer structure with two phases has existed for many years. However, it is intuitively perceptible that there is no physical possibility for an abrupt change between crystal and amorphous phase. There are experimental data providing the evidence for the additional component, an interfacial region with intermediate order between crystalline and amorphous [1–17]. Most of the experimental evidences for these intermediate regions were obtained using NMR and Raman spectroscopy. In those methods, three-phase model with crystalline, intermediate and amorphous regions is widely used for data interpretation. On the contrary, WAXS data from unoriented semicrystalline polymers are routinely approximated with two components – a broad halo corresponding to amorphous phase and several sharp peaks corresponding to the crystalline scattering. So far there is only a few experimental results obtained by WAXS, indicating a necessity to include an intermediate phase into the analysis of unoriented polymers [11,13,16]. The intermediate phase is more widely accepted to exist in oriented semicrystalline polymers.

This work is devoted to the WAXS analysis of the kinetics of isothermal and non-isothermal crystallization of various polyethylenes. At this stage of analysis, we discuss the approximation procedures for WAXS radial profiles and show the necessity of accounting for an additional intermediate phase. We discuss some general features of the kinetics of crystallization analysed with an additional intermediate phase. Moreover, we compare this approach with the traditional two-phase concept. The special interest

* Corresponding author. Tel.: +48 22 8261281x148; fax: +48 22 8269815.
*E-mail address:* psajk@ippt.gov.pl (P. Sajkiewicz).

0032-3861/$ - see front matter © 2004 Elsevier Ltd. All rights reserved.
doi:10.1016/j.polymer.2004.11.018

is the behavior of the intermediate phase during crystallization. The classical two-phase model applied commonly to the analysis of WAXS data for unoriented polymers seems to be only a rough approximation of the real polymer structure. The application of polyethylene as a model polymer is very convenient, since the amorphous halo is relatively well separated from the crystalline peaks. Additionally, as suggested by Baker and Windle [16], the thickness of the interfacial component in polyethylene is expected to be relatively large since the persistence of the planar zig-zag all-trans crystalline conformation beyond the crystalline environment is probably stronger than for polymer chains with helical crystalline conformation. The use of polyethylenes with various branch concentration as well as molecular weight allow the discussion of the effect of chain imperfections, such as branches, and ends of molecules, on a structure, especially on a content of the intermediate phase. There is still discussion in the literature on the role of chain imperfections in crystallization of polymers [18].

## 2. Experimental

### 2.1. Materials

Several linear low-density polyethylenes (LLDPE) synthesized by metallocene homogeneous catalysts supplied by Dow Chemical Co were investigated. They were synthesized using octene as comonomer resulting in hexyl branches. The details of the samples characteristics are listed in Table 1. In addition to LLDPEs, high-density polyethylene was also investigated.

### 2.2. Method

Wide-angle X-ray scattering (WAXS) measurements were performed using rotating anode X-ray generator and one-dimensional position sensitive counter to obtain WAXS profiles. Occasionally an imaging plate as a two dimensional (2D) detector [19] was used in order to assure that there is no preferred orientation in investigated samples. Temperature chamber was mounted in the X-ray apparatus. Samples were tightly covered with Al foil. Temperature history during experiments was controlled by means of a programmable temperature controller. The actual temperature of the sample was detected by a thermocouple mounted close to the sample. Two types of experiments were performed: isothermal crystallization and non-isothermal crystallization during cooling at a constant rate. The melt temperature kept before crystallization was 150 °C. Each profile was accumulated with an exposure time of 10 or 20 s, depending on the experimental conditions.

Table 1
Characteristics of PEs

| Sample code | $M_w$ ($\times 10^4$) | $M_n$ ($\times 10^4$) | Branch content ($CH_3$/1000 C) |
|---|---|---|---|
| L24 | 4.69 | 2.18 | 24.04 |
| H17 | 10.27 | 4.87 | 16.92 |
| L10 | 4.37 | 2.12 | 10.86 |
| H10 | 10.61 | 4.71 | 9.95 |
| H07 | 9.84 | 4.48 | 7.32 |
| HDPE | 43.71 | 1.64 | – |

### 2.3. Data evaluation

After subtraction of incoherent scattering, the radial profiles of X-ray scattering, $I(2\theta)$, were approximated by the sum of several Pearson VII functions

$$I(2\theta) = \sum_{n=1,2\ldots} f_n(2\theta) \tag{1}$$

Each of the $n$th Pearson VII function has the form

$$f_n(2\theta) = \frac{A_n}{\left[1 + 4\left(\frac{2\theta - 2\theta_{\max,n}}{w_n}\right)^2 (2^{1/m_n} - 1)\right]^{m_n}} \tag{2}$$

where $2\theta_{\max,n}$ is the diffraction angle at which $f_n(2\theta)$ reaches the maximum value, $A_n$ is the intensity at $2\theta = 2\theta_{\max,n}$, $w_n$ is the full width at half maximum, and $m_n$ is the shape parameter of the $n$th function. When $m_n = 1$, the Pearson VII distribution reduces to the Cauchy, while as $m_n$ approaches infinity the Pearson distribution approaches the Gaussian form. The spacing $d$ between $(hkl)$ planes in crystals and the approximate value of the most probable interatomic distance in the intermediate and amorphous regions was determined from the position of the maximum $2\theta_{\max,n}$ using Bragg law

$$d = \frac{k\lambda}{2 \sin \theta_{\max,n}} (k = 1, 2\ldots) \tag{3}$$

Degree of weight averaged crystallinity $x$ at particular temperature was calculated from

$$x = \frac{\sum_{n=3}^{n=4} \int_{s_{n,1}}^{s_{n,2}} f_n(s) s^2 \, \mathrm{d}s}{\sum_{n=1}^{n=4} \int_{s_{n,1}}^{s_{n,2}} f_n(s) s^2 \, \mathrm{d}s} \tag{4}$$

where $s = (2 \sin \theta)/\lambda$ is the scattering vector, indices 1 and 2 denote the Pearson VII function for amorphous halo and intermediate phase, respectively, and index 3 and 4 are related to (110) and (200) reflections. The scattering vectors $s_{n,1}$ and $s_{n,2}$ are the lower and upper bounds, below and above which the diffraction intensity becomes effectively negligible, respectively. In the case of the two-phase model there is no component of the intermediate phase.

The error of measurements was estimated as a standard deviation from the mean value by repeating the same experiment several times using new sample every time. Debye–Waller temperature correction was neglected.

Additionally, a few DSC experiments were performed in order to analyse the kinetics of non-isothermal

crystallization and compare it with data obtained by WAXS. The Perkin–Elmer apparatus model Pyris-1 was used. Weight crystallinity $x$ was determined as the absolute value from DSC thermograms using equation

$$x = \frac{\int_T^{T_m} \left(\frac{dQ}{dt} / \frac{dT'}{dt}\right) dT'}{m\Delta h_c} \quad (5)$$

where $dQ/dt$ is the rate of evolution of crystallization heat, which after dividing by cooling rate, $dT'/dt$, is integrated in the temperature range between the melting temperature, $T_m$, and the actual temperature, $m$ is the sample mass, and $\Delta h_c$ is the enthalpy difference per unit mass between amorphous and completely crystalline polymer assumed as 293 J/g [20].

## 3. Results

### 3.1. Approximation using two-phase model

Fig. 1 illustrates the typical WAXS profiles registered during isothermal crystallization at elevated temperatures (shown by data points) and approximated profiles using two-phase model (solid line, broken lines labeled A and C, representing net profile, profiles from amorphous and crystal regions, respectively). It is seen that in the case of partially crystalline samples there is a part of scattering that is unaccounted for resulting in poor quality of the two-phase approximation.

In addition to the problem of approximation quality of a singular WAXS profile as pointed out above, the strongest evidence for the inapplicability of the two-phase model comes from the analysis of a sequence of WAXS patterns during crystallization. In such an analysis, the application of two-phase model results in unexpected time (Fig. 2) or temperature dependence (Fig. 3) of the angular position, $2\theta_{max}$, and the width, $w$, of the function fitting of amorphous halo during crystallization. In the case of isothermal process, crystallization is accompanied by an increase of both parameters of amorphous fitting function above the constant level observed before the start of crystallization (Fig. 2). It is expected that the amorphous halo position as well as the width should remain constant with time in isothermal crystallization, as the position and width of crystalline reflections do. In the case of non-isothermal crystallization, the position of maximum (Fig. 3a) and the width of the amorphous fitting function (Fig. 3b) shift from the linear temperature dependence obtained in the range of temperatures where crystallization does not occur. The trends shown in Figs. 2 and 3 are typical for all investigated polyethylenes. Similar behavior was observed by McFaddin et al. [11] during heating of branched polyethylenes. The linear temperature dependence of the spacing and hence the angular position (considering the limited change in the spacing as a function of temperature) is expected as a result

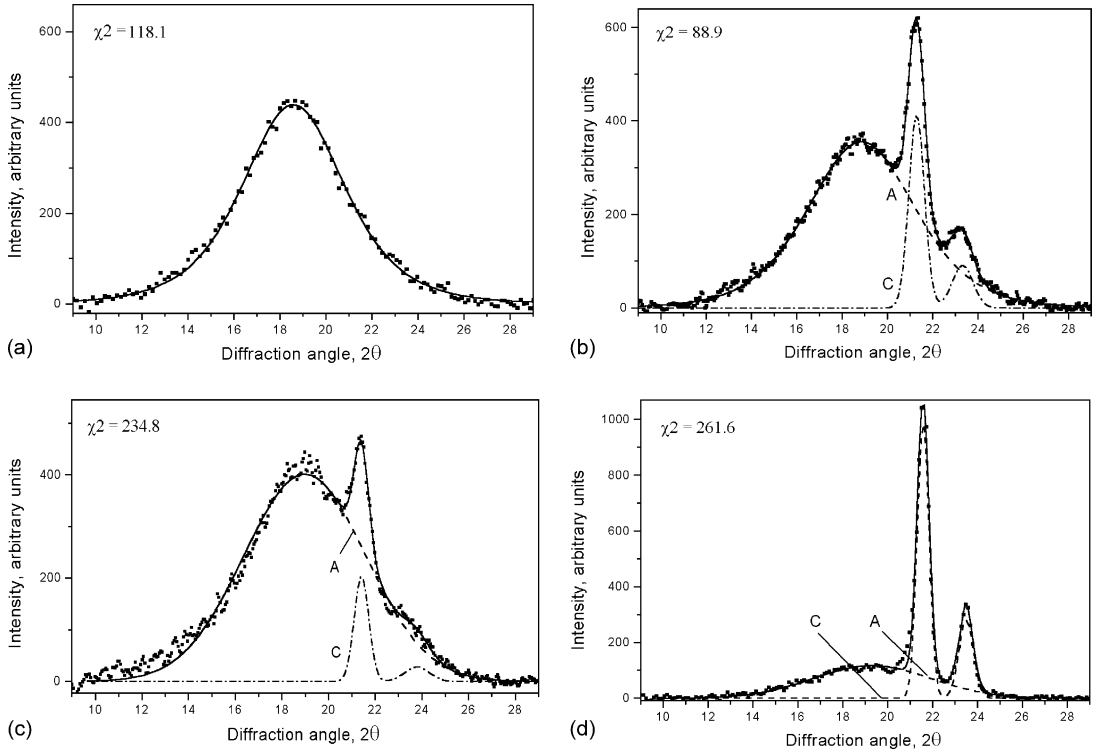


Fig. 1. Approximation of WAXS profiles using two-phase model (filled squares—experimental points, broken line (A)—amorphous halo, broken line (C)—crystalline peaks, solid line—net profile). Chi-square parameter, $\chi^2$, was also indicated in the figure: (a) LLDPE H10, 1 min at 98 °C, (b) LLDPE H10, 26 min at 98 °C, (c) LLDPE L24, 34 min at 82 °C, (d) HDPE, 130 min at 124 °C.

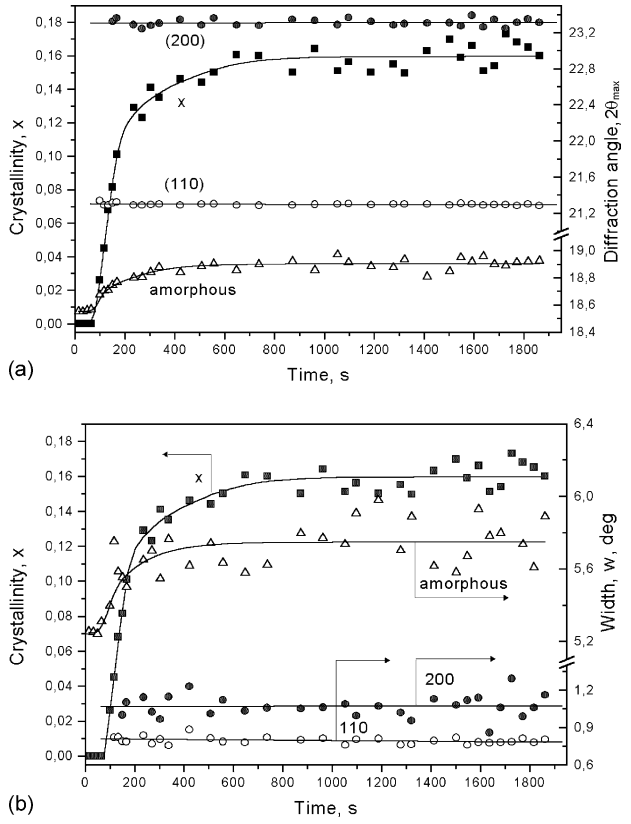


Fig. 2. Crystallinity, $x$, and the angular position at the maximum, $2\theta_{max}$, (a) and the width $w$, (b) of amorphous and crystal fitting functions during isothermal crystallization of LLDPE H10 at 98 °C. Analysis using two-phase model.

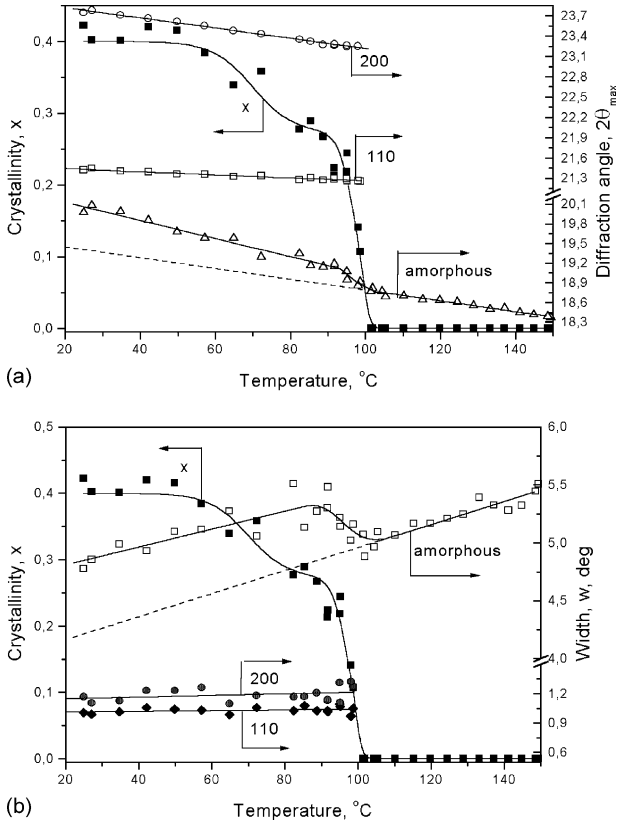


Fig. 3. Crystallinity, $x$, and the angular position at the maximum, $2\theta_{max}$, (a) and the width, $w$, (b) of amorphous and crystal fitting functions during non-isothermal crystallization of LLDPE H10 at cooling rate 4°/min. Analysis using two-phase model.

of thermal contraction. The linear plot of the angular position as a function of temperature was demonstrated by McFadden [11] for a liquid polyethylene and alkanes.

From the above, it can be concluded that the WAXS profiles of partially crystalline samples cannot be fitted using the traditional two-phase approach. The application of this method to the analysis of crystallization kinetics leads to unexpected behavior of the parameters of amorphous function.

### 3.2. Approximation using three-phase model

Fig. 4 shows the same experimental WAXS profiles (shown by data points) as in Fig. 1 approximated now using amorphous component (A), crystalline component (C) and the additional function for the intermediate component (M).

It is evident that the accounting for the intermediate phase improves the quality of approximation of WAXS profiles. The angular position and the width of the peak from the intermediate phase are optimized between the values of the amorphous halo and 110 reflection as a result of the least square minimization. It indicates that the most probable spacing and the content of structural defects and/or size of the intermediate regions are between those of amorphous and crystalline phases. The angular position varies among the investigated polyethylenes. We found the correlation between the angular position and the width of the peak from the intermediate phase. In the case of HDPE as well as LLDPEs with low branch content and low molecular weight (e.g. L10) the angular position of the peak of the intermediate phase is very close to the position of 110 reflection and the width is relatively low (Table 2). With increasing branching content and molecular weight, the peak of intermediate phase shifts toward amorphous halo and it becomes wider. It indicates that an increase of the branching content and molecular weight makes the structure of the intermediate material closer to the amorphous structure than in the case of low-branched LLDPEs.

Application of the three-phase model to the analysis of crystallization kinetics leads to the physically reasonable time and temperature dependencies of the parameters of amorphous halo (e.g. the angular position and width of amorphous halo do not change during isothermal crystallization while in the case of non-isothermal crystallization their temperature dependencies tend to remain linear). However, considering a partial overlapping of the reflections and problems with the convergence of numerical approximation we decided for the sake of efficiency to reduce the number of fitting parameters by putting constraints on the amorphous fitting function. Such

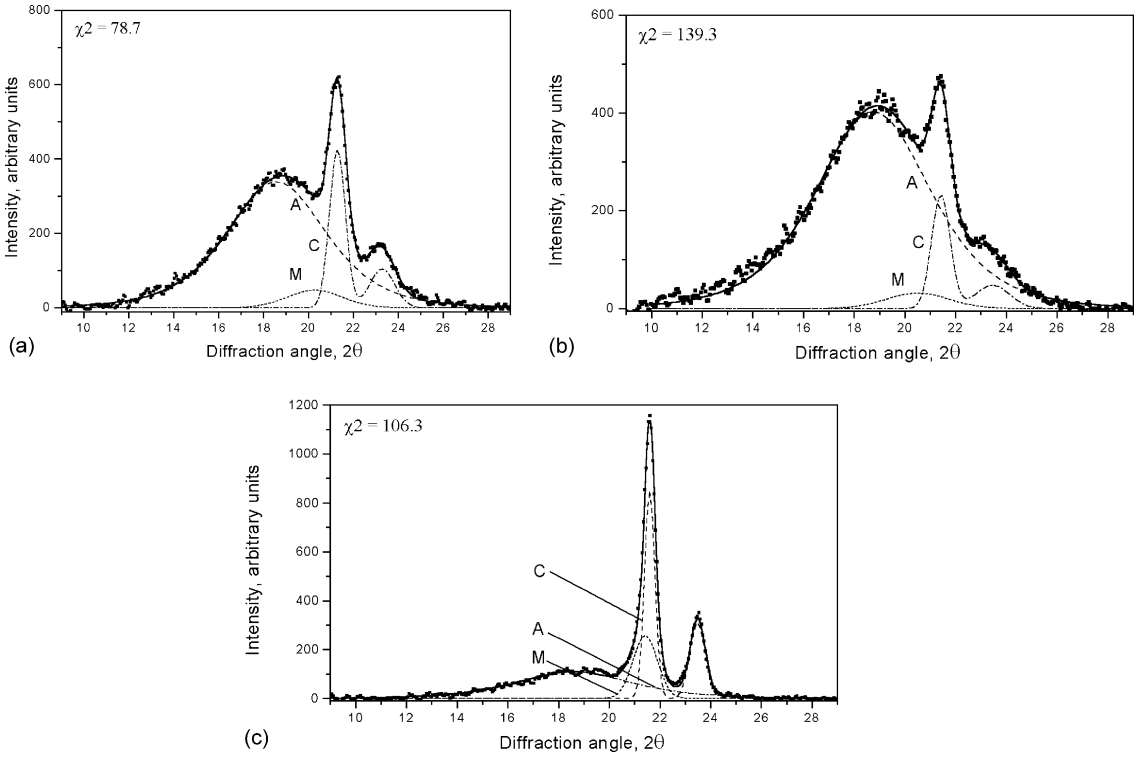


Fig. 4. Approximation of WAXS profiles of partially crystalline samples using three-phase model (filled squares—experimental points, solid lines—net profiles obtained from amorphous halo (A), intermediate component (M), and crystalline peaks (C)). Chi-square parameter, $\chi^2$, was also indicated in the figure: (a) LLDPE H10, 26 min at 98 °C, (b) LLDPE L24, 34 min at 82 °C, (c) HDPE, 130 min at 124 °C.

constrains were drawn from the WAXS analysis of the amorphous halo in the time (temperature) range before the start of crystallization. In the case of isothermal crystallization we assumed that the angular position, width as well as shape parameter of the amorphous halo depend only on temperature but not on time, e.g. have the same values as that before crystallization at a given temperature. In the case of non-isothermal crystallization the angular position, width, and shape parameter of amorphous halo were determined from the linear extrapolation of the plot of

Table 2
Crystallinity and the parameters of WAXS profiles in isothermal crystallization

| Sample/temperature (°C) | Parameters | | | | | | | | |
|---|---|---|---|---|---|---|---|---|---|
| | $2\theta_{max,am}$ | | $w_{am}$ | | $2\theta_{max,int}$ | $w_{int}$ | $r_{i/c}$ | Crystallinity | |
| | 3-Phase | 2-Phase[a] | 3-Phase | 2-Phase[a] | | | | 3-Phase[a] | 2-Phase [a] |
| L24/82 | 18.75 | 19.00 | 5.38 | 5.90 | 20.50 | 2.2 | 0.35 | 0.090 | 0.079 |
| H17/85 | 18.76 | 18.94 | 5.50 | 5.65 | 20.02 | 2.5 | 0.36 | 0.140 | 0.121 |
| L10/104 | 18.57 | 18.86 | 5.35 | 5.86 | 21.13 | 1.4 | 0.49 | 0.151 | 0.160 |
| H10/98 | 18.58 | 18.90 | 5.28 | 5.77 | 20.60 | 2.3 | 0.33 | 0.175 | 0.161 |
| H07/101 | 18.60 | 19.02 | 5.35 | 5.98 | 20.80 | 2.4 | 0.42 | 0.205 | 0.189 |
| HDPE/124 | 18.58 | 19.41 | 5.51 | 6.51 | 21.35 | 0.84 | 0.58 | 0.351 | 0.493 |

| Sample/temperature (°C) | Parameters | | | | | | | |
|---|---|---|---|---|---|---|---|---|
| | $2\theta_{max,110}$ | | $2\theta_{max,200}$ | | $w_{110}$ | | $w_{200}$ | |
| | 3-Phase | 2-Phase | 3-Phase | 2-Phase | 3-Phase | 2-Phase | 3-Phase | 2-Phase |
| L24/82 | 21.40 | 21.40 | 23.45 | 23.57 | 0.72 | 0.68 | 1.26 | 1.21 |
| H17/85 | 21.33 | 21.33 | 23.33 | 23.36 | 0.75 | 0.76 | 1.26 | 1.08 |
| L10/104 | 21.36 | 21.34 | 23.33 | 23.35 | 0.57 | 0.64 | 1.08 | 0.86 |
| H10/98 | 21.31 | 21.29 | 23.28 | 23.31 | 0.66 | 0.67 | 1.12 | 0.91 |
| H07/101 | 21.36 | 21.35 | 23.34 | 23.33 | 0.66 | 0.67 | 1.03 | 0.85 |
| HDPE/124 | 21.46 | 21.42 | 23.31 | 23.33 | 0.38 | 0.49 | 0.61 | 0.54 |

[a] The values at the end of crystallization.

them vs. temperature determined in the melt. Therefore, the only parameter of amorphous halo allowed to change during iso- and non-isothermal crystallization is the height of the maximum.

It is quite probable that molecular segregation in terms of molecular weight and branches can occur during isothermal crystallization. However, we believe that this segregation does not essentially affect the peak position of amorphous halo as evidenced by a paper of McFaddin et al. [11].

### 3.3. Kinetics of crystallization

The general comparison of the kinetics of crystallization analysed using two- and three-phase model as well as the influence of the model on some structural characteristics will be given below.

#### 3.3.1. Isothermal crystallization

Typical kinetics of isothermal crystallization analysed using three-phase model is illustrated in Fig. 5.

It is seen that the changes of weight-fraction of crystalline and intermediate phases during isothermal crystallization can be described by the sigmoidal function. Crystallinity determined using three-phase model differs from that obtained using traditional two-phase concept (Fig. 5). The differences in crystallinity depend on the position of the peak of intermediate phase in relation to the positions of the amorphous halo and crystalline reflections. In the case of HDPE as well as LLDPEs with low branching content and low molecular weight (e.g. L10), the close position of the peak of the intermediate phase to the (110) reflection results in high ratio of the intermediate phase to the crystalline phase content ($r_{i/c}$) (Table 2). This 'consumption' of crystalline peak by the intermediate component leads to the lower crystallinity as obtained by three-phase model than that from two-phase approach, even by 30% in the case of HDPE (Table 2). For LLDPEs with higher branch content and higher molecular weight (e.g. H17) the peak of intermediate phase shifts toward amorphous halo 'consum-consuming' thus this part of scattering rather than

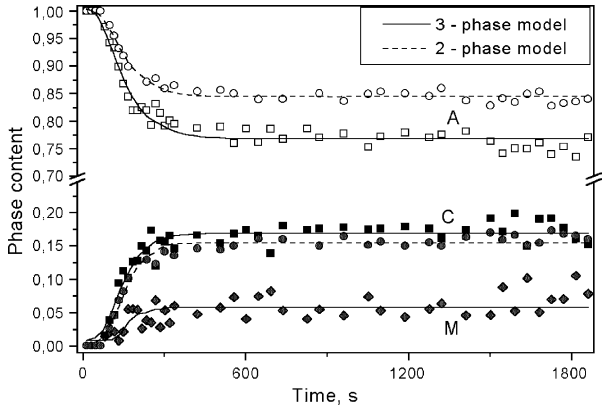


Fig. 5. Kinetics of isothermal crystallization of LLDPE H10 at 98 °C (A—amorphous phase, C—crystalline phase, M—intermediate phase).

crystalline part. For those polymers crystallinity obtained by three-phase model is higher than that from two-phase approach by 9 to 16% (Table 2). The same trend is observed for H10 as shown in Fig. 5.

Our results indicate that the choice of the model affects not only the parameters of amorphous halo but also those of crystalline reflections. As discussed earlier, there is the apparent widening and shift of the amorphous function toward higher angles when two-phase model is applied. In the case of parameters of crystalline reflections it is seen that the most evident effect concerns the width of the (200) peak. For all polethylenes the width of (200) reflection determined using two-phase model is lower than that obtained from three-phase approach. The effect of the applied model on the width of (110) reflection is seen only for HDPE and LLDPE with low branch content and molecular weight (L10), having the reflection from the intermediate phase very close to (110) crystalline peak. In those polyethylenes, the width of (110) reflection determined using two-phase model is higher than that obtained using three-phase approach. There is also some difference in the angular positions of crystalline peaks determined using two- and three-phase models. This difference is mostly evident for (200) reflection (Table 2).

#### 3.3.2. Non-isothermal crystallization

Fig. 6 illustrates the changes in weight fraction of each phase analysed using three- and two-phase model during non-isothermal crystallization at one of the applied cooling rate.

The analysis of crystallization kinetics shows two-stage crystallization of LLDPEs. In addition to the high-temperature region (stage I comprised of $I_1$ and $I_2$ in Fig. 6), where the major part of crystallinity develops, there is also an additional low temperature crystallization that starts in the range between 45 and 60 °C, depending on the branch content and the molecular weight (stage II in Fig. 6). According to the opinions existing in the literature (e.g. [21]) the high temperature crystallization occurs from segments with low concentration of branches, while the lower temperature region involves crystallization of segments with high content of branches. The high temperature transition can be further divided into two regions. In the first one, that can be attributed to primary crystallization, major part of crystallinity develops with relatively high rate (stage $I_1$ in Fig. 6), while in the second one being probably a process of secondary crystallization - additional crystallization occurs at a lower rate (stage $I_2$ in Fig. 6). It is seen in Fig. 6 that the primary crystallization is ended with a saturation of crystallinity. The dependence of crystallinity on the applied model is stronger for LLDPEs with higher branch content (Fig. 6d). For HDPE and LLDPEs with low branch content, the fraction of crystalline phase in both models is very close one to other (Fig. 6a and b). The largest difference in the content of crystalline phase as analysed by both models is seen in the range of secondary crystallization in the high temperature region ($I_2$) as well as in the low

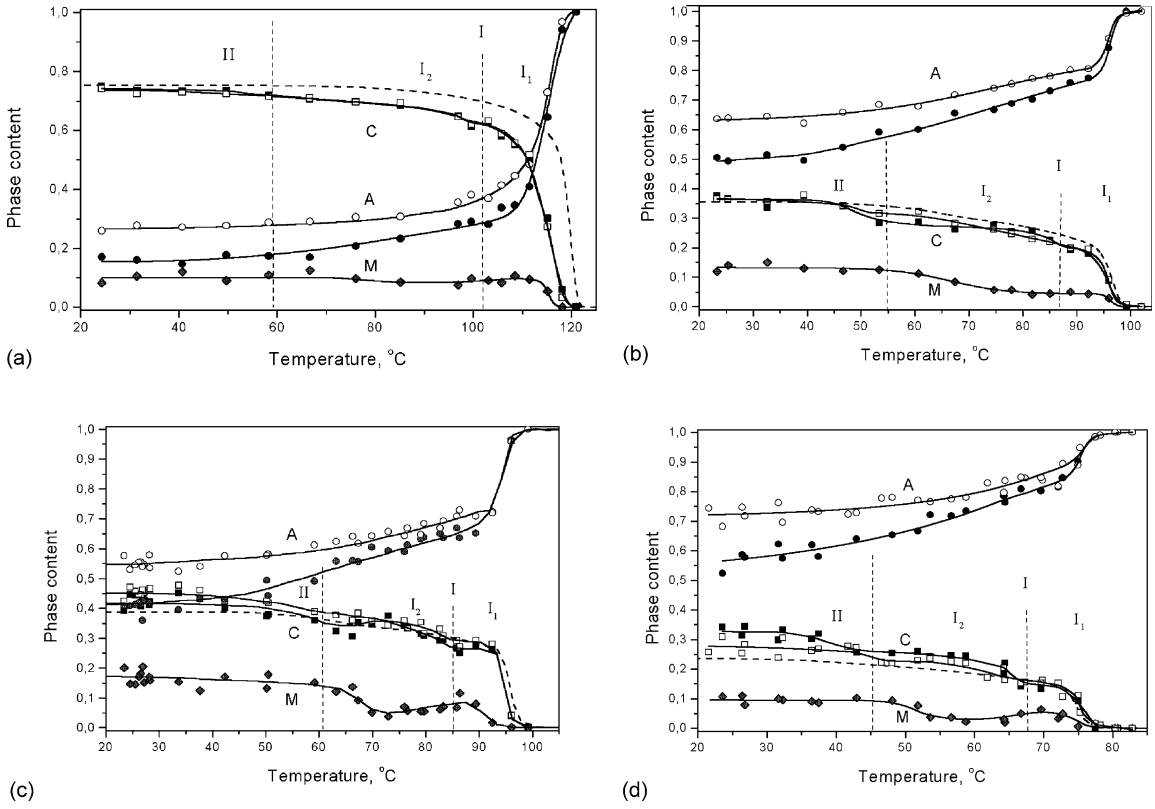


Fig. 6. Changes in weight fraction of each component (A—amorphous, C—crystalline, M—intermediate phase) during cooling at 4 °C/min. Open points -two-phase model, solid points—three-phase model. Dashed line—DSC data. (a) HDPE, (b) LLDPE H10, (c) LLDPE L10, (d) LLDPE L24.

temperature range crystallization (II). Both processes are more clearly seen when three-phase model is applied. Even in the case of HDPE analysed with three-phase model it is quite probable that there is small additional crystallization in the region of low temperature transition (II) (Fig. 6a). It is seen in Fig. 6 that in the case of non-isothermal crystallization the choice of the model affects very clearly the content of amorphous phase.

Simultaneous analysis of the content of crystalline and intermediate phases provides interesting information on the nature of crystallization. First it is seen that the formation of crystals from amorphous phase at the beginning of the process (primary crystallization, $I_1$) is accompanied by formation of the regions with intermediate order that most probably are associated with imperfection on a crystal surface. In the region of secondary crystallization (stage $I_2$ in Fig. 6) there is a slight decrease in the content of intermediate phase, indicating that secondary crystallization occurs not only from amorphous phase but also from the regions with intermediate order. Regarding the low-temperature crystallization (stage II in Fig. 6) it is seen that an increase of crystallinity is preceded by an increase of the content of intermediate phase. This increase of the content of intermediate phase is accompanied by constant or even decreasing content of crystalline phase. Such a change in phase content in the low temperature region suggests that this transition is a kind of reorganization occurring in crystal phase via intermediate phase.

The comparison of the WAXS results with those obtained using DSC method that is commonly applied for the analysis of crystallization kinetics shows the difference between both methods (Fig. 6). It is seen in Fig. 6 that the difference between DSC and WAXS crystallinities is not the same for all investigated polyethylenes. In the case of HDPE, WAXS crystallinity determined using 3-phase approach is indeed below the DSC value while in the case of highly branched polyethylenes WAXS crystallinity is higher than DSC one. For LLDPEs with lower branch content, WAXS and DSC crystallinities are quite similar. So we expect that there is some systematic trend but at this stage of analysis we would not like to discuss deeply this aspect.

Like in the case of isothermal crystallization, the applied model affects the angular positions as well as width of reflections during non-isothermal crystallization. The strongest effect is observed for amorphous phase. When the two-phase model is applied, the fitting function for amorphous halo tends to cover the part of scattering related to the intermediate material. It results in a shift toward higher angles as well as broadening of amorphous halo compared to the values obtained using three-phase model (Figs. 3 and 7). In the case of crystalline reflections the angular position

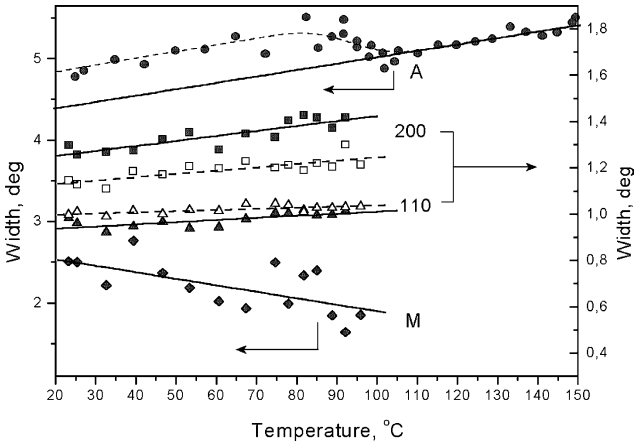


Fig. 7. The width of reflections from amorphous, intermediate and crystalline (110 and 200) phases of LLDPE H10 as a function of temperature. Solid lines—three-phase model, dashed lines—two-phase model. Cooling rate 4 °C/min.

and the width depend on the applied model practically only in the case of (200) reflection. Fig. 7 illustrates the difference in the width of (200) reflection determined using two- and three-phase models. It is seen that the application of two-phase model leads to the underestimation of the width of (200) reflection.

It is worth noticing that the temperature dependence of the width of reflections from intermediate phase is opposite to that observed for crystalline and amorphous one. As it is seen in Fig. 7 the width of intermediate phase reflections increases during cooling. This trend indicates that the mean size and/or perfection of the regions of intermediate material are reduced during crystallization.

## 4. Summary and discussion

Our results show that the accurate description of a structure of polyethylenes needs the application of the third intermediate phase in addition to the crystalline and amorphous phases. The position and the width of the WAXS reflection from the intermediate phase is between the position of the amorphous halo and the crystalline reflections, indicating thus that its structure is between the structure of the amorphous and crystalline phases. In the case of linear polyethylene, the angular position of the peak of the intermediate phase as well as its width is relatively close to the parameters of (110) reflection of crystal phase. With increasing branch content and molecular weight the structure of the intermediate phase becomes more similar to the structure of the amorphous phase.

There are two pieces of evidence that the application of two-phase model to the quantitative analysis of the WAXS profiles of various polyethylenes is not an appropriate method. The first one is a poor quality of approximation of experimental WAXS profiles, which is particularly evident at higher temperatures. The error of approximation using two-phase model diminishes with decreasing temperature due to position of amorphous halo becoming closer to that of the reflections from crystal (Fig. 8).

The second evidence for a weakness of two-phase model is clearly seen from the analysis of the parameters of amorphous halo during crystallization. When crystallization is started in isothermal or non-isothermal mode, an attempt to apply two-phase model results in a shift of the angular position and the width (Figs. 2 and 3) of the amorphous fitting function above the anticipated values which are obtained by extrapolating the respective values from those in the melt. This is caused by the fact that the amorphous fitting function tries to cover a peak of the intermediate phase that appear between amorphous halo and (110) reflection of crystalline phase.

Consideration of the intermediate phase provides additional information on the nature of crystallization itself. The role of intermediate phase seems to be most important during secondary crystallization in high temperature region as well as during low temperature additional crystallization.

Taking into account that the three-phase model is an adequate model for the structure of investigated polyethylenes, it is important to discuss the error related to application of two-phase model that is widely used for the analysis of a polymer structure. For the analysis of crystallization kinetics, the crucial parameter is a content of crystalline phase. Although the strongest influence of the applied model is observed for the weight fraction of amorphous phase, there is also some effect on the weight fraction of crystalline phase. This error varies with the type of polyethylene as well as with conditions of crystallization. The error in crystallinity determination is mostly evident in isothermal crystallization at elevated temperatures where the separation between the amorphous halo and crystalline peaks is relatively large. The sign of the error can be either plus or minus depending on the relative position of the reflection of intermediate phase. In the case of linear polyethylene and LLDPE with low branch content and molecular weight, the position of the intermediate phase

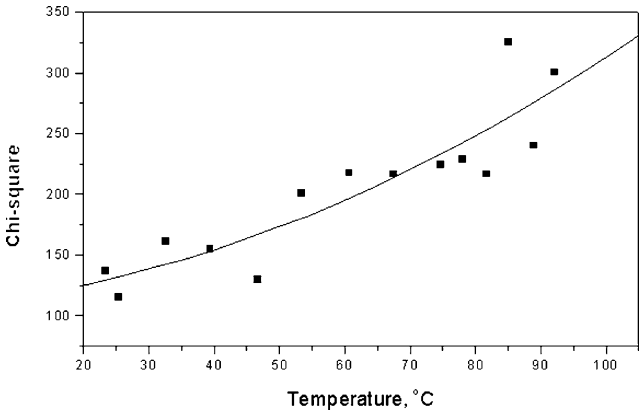


Fig. 8. The error of approximation (chi-square) using two-phase model of a sequence of WAXS profiles registered during non-iosthermal crystallization of H10 sample. Cooling rate 4 °C/min.

reflection is close to that of the (110) crystalline peak, resulting in overestimation of crystallinity in two-phase model (Table 2). Opposite relation is seen for LLDPEs with higher branch content and molecular weight for which the peak position of intermediate component is much closer to the amorphous halo, leading to underestimation of crystallinity in two-phase model (Table 2).

Application of two-phase model leads also to erroneous values of other structural parameters like the characteristic spacing as well as a perfection and/or size of regions of particular phase as determined by WAXS. In the case of amorphous phase, the application of two-phase model leads to an overestimation of the peak position (underestimation of the characteristic spacing) by 2 to 4% as well as the width by 10 to 20% depending on the used polymer and crystallization conditions. In the case of crystalline phase, the most important error is related to the width of (200) reflection. The width of (200) reflection determined using two-phase model is lower than that obtained using three-phase approach, even by 20%.

In our opinion, there are two methods of the analysis of WAXS profiles using three-phase model. The first one is the approximation of WAXS profiles with the adequate number of functions, including that for intermediate component without any constraints put on the parameters. This process should result in free generation of the parameters of all peaks including that of intermediate phase in the course of numerical optimisation. The second possibility is the numerical optimisation with the constraints put on the amorphous halo, allowing thus the reduction of number of fitting parameters. This method needs additional data on the amorphous phase, which can be obtained by registration of the sequence of WAXS patterns in the range of time or temperature before the start of crystallization.

## Acknowledgements

The work was conducted at Kyoto University in the frame of the Polish - Japanese scientific cooperation with financial support provided by the State Committee for Scientific Research (Komitet Badań Naukowych) (project R-16 077). The authors would like to gratefully acknowledge Prof. Dr A. Ziabicki for his encouragement through this work.

## References

[1] Strobl GR, Hagedorn W. . J Polym Sci, Polym Phys Ed 1978;16:1181.
[2] Tanabe Y, Strobl G, Fisher EW. Polymer 1986;27:1147.
[3] Glotin M, Mandelkern L. Coll Polym Sci 1982;260:182.
[4] Murthy NS, Minor H. Polymer 1990;31:996.
[5] Fu Y, Annis B, Boller A, Jin Y, Wunderlich B. J Polym Sci, Polym Phys Ed 1994;32:2289.
[6] Kitamaru R, Horii F, Murayama K. Macromolecules 1986;19:636.
[7] Cheng J, Fone M, Reddy VN, Schwartz KB, Fisher HP, Wunderlich B. J Polym Sci, Polym Phys Ed 1994;32:2683.
[8] Axelson DE, Mandelkern L, Popli R, Mathieu P. J Polym Sci, Polym Phys Ed 1983;21:2319.
[9] Gerum W, Hohne GWH, Wilke W. Macromol Chem Phys 1996;197:1691.
[10] Packer KJ, Poplett IJF, Taylor MJ. J Chem Soc Faraday Trans I 1988;84:3851.
[11] McFaddin DC, Russel KE, Wu G, Heyding RD. J Polym Sci, Polym Phys Ed 1993;31:175.
[12] Olcak D, Sevcovic L, Mucha L. Acta Phys Slov 2000;50:259.
[13] Monar K, Habenschuss A. J Polym Sci, Polym Phys Ed 1999;37:3401.
[14] Kristiansen PE, Hansen EW, Pedersen B. Polymer 2001;42:1969.
[15] Jinlong Ch, Fone M, Reddy VN, Schwartz KB, Fisher HP, Wunderlich B. J Polym Sci, Polym Phys Ed 1994;32:2683.
[16] Baker AME, Windle AH. Polymer 2001;42:667.
[17] Tashiro K, Sasaki S. Prog Polym Sci 2003;28:451.
[18] Kim MH, Phillips PJ, Lin JS. J Polym Sci, Polym Phys Ed 2000;38:154.
[19] Hashimoto T, Okamoto S, Saijo K, Kimishima K, Kume T. Acta Polym 1995;46:463.
[20] Wunderlich B. Crystal melting. Macromolecular physics. vol. 3. New York: Academic Press; 1980.
[21] Wilfong DL, Knight GW. J Polym Sci, Polym Phys Ed 1990;28:861.